

## Multiple-scattering $X\alpha$ molecular-cluster model of complex defects in semiconductors: Application to $\text{Si:P}_2$ and $\text{Si:P}_2^+$ systems

M. J. Caldas, J. R. Leite, and A. Fazzio

*Instituto de Física, Universidade de São Paulo, Caixa Postal 20516, São Paulo, SP, Brazil*

(Received 19 August 1981)

In this work we study the effect of a pair of nearest-neighbor substitutional P atoms in the Si lattice, with the use of a molecular-cluster model within the formalism of the self-consistent-field multiple-scattering  $X\alpha$  method. The complex is studied in neutral- and positive-charge states. It is found that the complex defect introduces two levels in the crystal band gap, one singly degenerate and fully occupied in the neutral charge state, and one doubly degenerate, slightly higher in energy and unoccupied. Analysis of the localization of the wave function shows that the defect cannot be studied within the shallow-donor effective-mass theory. The results are compared with EPR data, and it is suggested that a pseudo-Jahn-Teller-effect may occur.

### I. INTRODUCTION

Point defects and impurities in covalent semiconductors have been objects of interest for a long time, from both experimental and theoretical points of view.<sup>1-4</sup> As a result, there is at present a wealth of experimental data, of which a great part still lacks satisfactory theoretical analysis.

Complexes of point defects and impurities can be formed in heavily doped semiconductors or during irradiation processes,<sup>1,5</sup> and may also appear as native defects in the lattice.<sup>6</sup> Defect complexes have been studied for many years now through different experimental techniques.<sup>7-11</sup> Some of them are actually better characterized than the isolated impurity or point defect: a typical example is the divacancy in Si, which is more conveniently studied than the neutral monovacancy since the latter is mobile at room temperature.<sup>11</sup>

The electronic structure of a system of interacting impurities and/or defects, due to its molecular character, may differ considerably from that of the isolated point defect. In a semiconductor heavily doped with shallow donors, for example, one of the major effects of donor interactions is to delocalize the isolated impurity wave function, giving rise to a metal-insulator transition.<sup>5</sup> The effects related to these interactions have long been receiving a great deal of attention. Besides idealized models as those of Anderson and Hubbard, donor-cluster models have been used to interpret experiments such as optical absorption and magnetic susceptibility in doped semiconductors.<sup>12</sup> The common feature of these donor-cluster approximations is the

validity of the shallow-donor effective-mass theory.<sup>13</sup> In the limit of strongly interacting impurities this assumption is no longer valid, and we are faced with deep-level, accidental deep-level, resonance, and hyper-deep-level problems.

The simplest "deep-level" complex can be formed with pairs of defects first neighbors in the lattice, such as the divacancy, a vacancy and a substitutional impurity, two substitutional impurities, a di-interstitial, etc. Even pairs of shallow-donor impurities may turn out to be deep traps in the limit of nearest-neighbor lattice-site separation. In spite of the large amount of experimental data available for the class of deep-level complexes, hitherto few attempts have been made to interpret these data in terms of realistic theoretical models. We recognize that these systems represent a more complicated problem than the isolated defect, which themselves remain a major challenge. Work to date includes the application of the extended Hückel theory (EHT) to the study of hydrogen-related complexes and the positive divacancy in Si.<sup>14-16</sup> Impurity vibrations due to defect complexes in Si have been studied through the EHT technique and in zinc-blende-type crystals through the Green's function theory.<sup>15,17</sup> Divacancies in cubic silicon carbide have been described by a tight-binding model.<sup>18</sup> A suitable empirical version of this model has been utilized recently to investigate chemical trends in nearest-neighbor substitutional defect pairs in GaAs, GaP, and in P-rich  $\text{GaAs}_{1-x}\text{P}_x$ .<sup>19,20</sup> Previously, Jaros and Brand applied the pseudopotential method to the study of the divacancy and the gallium vacancy-oxygen pair

in GaAs.<sup>21</sup>

In this paper we investigate the electronic structure of the nearest-neighbor substitutional pair of P in Si within the framework of the self-consistent-field multiple-scattering (MS)  $X\alpha$  molecular cluster model.<sup>22</sup> To our knowledge, this is one of the first attempts to perform a self-consistent calculation for a complex crystal defect. It has been verified that charge-relaxation effects around the defects cannot be neglected in a realistic description of a point defect or a complex.<sup>16,23</sup> The P pair complex in Si is considered here in neutral ( $\text{Si:P}_2$ ) and positive ( $\text{Si:P}_2^+$ ) charge states. The results presented in the paper were obtained through the study of a 20-atom cluster; the boundary-condition problem associated with the surface dangling bonds is solved according to a proposal of Fazzio, Leite, and De Siqueira.<sup>24</sup> The results of the calculations are compared with the available electron paramagnetic resonance (EPR) data taken from electron-irradiated P-doped Si.<sup>25</sup>

## II. MS $X\alpha$ MOLECULAR CLUSTER MODEL

### A. Perfect crystal

According to the molecular cluster model, the electronic structure and related properties of a defect or impurity in the lattice are determined from the solutions of the Schrödinger equation for a selected cluster of host atoms surrounding the defect. The use of the MS technique permits the calculation to be carried out to self-consistency. In this case, suitable boundary conditions must be imposed at the cluster surface. The undesirable "dangling-bond" effects can be avoided by saturating the surface atoms of the cluster with hydrogen atoms,<sup>26–28</sup> or by transferring the electrons filling dangling bonds to a sphere surrounding the cluster (Watson sphere).<sup>24,29</sup> This latter procedure is adopted by us.

In order to locate the impurity level relative to the band edges of the crystal, the bulk solid is simulated by a cluster of Si atoms. The  $\text{Si:P}_2$  and  $\text{Si:P}_2^+$  systems are then simulated by replacing two nearest-neighbor Si atoms by two P atoms. The 20-atom cluster used for the studies is schematically shown in Fig. 1. The center of the cluster lies halfway between the two central atoms. The clusters are indicated by  $20\text{Si}$  and  $18\text{Si} + \text{P}_2$ ,  $18\text{Si} + \text{P}_2^+$ , for the bulk and the complexes, respectively. To solve the one-electron Schrödinger

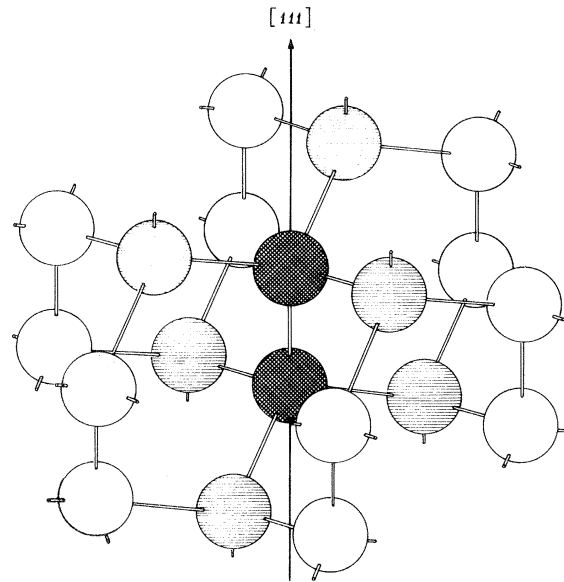


FIG. 1. Schematic representation of the 20-atom clusters used to simulate the bulk, the  $\text{Si:P}_2$ , and  $\text{Si:P}_2^+$  complexes. As a bond-centered cluster it comprises three shells of equivalent atoms, in  $D_{3d}$  symmetry. The first, second, and third shells have two, six, and 12 atoms, respectively.

equation we use the MS method within the standard muffin-tin approximation for the molecular potential. The method has been widely used in studies of the electronic structure of molecular species and atomic clusters.<sup>22</sup> The muffin-tin atomic spheres are chosen so as to touch each other without overlapping, and the value  $5.431 \text{ \AA}$  is assumed for the Si lattice constant.<sup>30</sup> The whole cluster is surrounded by an outer sphere (Watson sphere) touching the cluster surface atomic spheres. The Slater local approximation to the exchange-correlation potential  $X\alpha$  is used, with the atomic  $\alpha$  values reported by Schwarz.<sup>31</sup> We adopted the  $\alpha$  value of Si for the interatomic and outer regions. In the partial wave expansions of the wave function we have used up to  $l=2$  for the outer region and first-shell atomic spheres and up to  $l=1$  for the remaining atomic spheres, where  $l$  is the angular momentum index.

Symmetry assignments for the energy levels of the 20-atom clusters were made according to the irreducible representations of the  $D_{3d}$  point group. In Si the chemical bonds between one atom and its four neighbors are completely saturated by eight electrons through  $sp^3$  hybridizations; thus, the following molecular orbitals can be formed from the directed bonds in the 20-atom cluster:

$$\begin{aligned}
 \text{first shell: } & 1a_{1g}, \\
 \text{second shell: } & 1a_{1g} + 1e_g + 1a_{2u} + 1e_u, \\
 \text{third shell: } & 2a_{1g} + 1a_{2g} + 3e_g + 2a_{1u} \\
 & + 1a_{2u} + 3e_u.
 \end{aligned} \tag{1}$$

Therefore, from the total of 80 valence electrons in the cluster, 30 are filling dangling bonds; these electrons are then transferred to the Watson sphere.<sup>24</sup> In order to assess the influence of the size of the cluster on the results, calculations of the electronic structure of an 8-atom cluster have also been performed. This cluster 8Si has the two atoms of the first shell completely saturated by 14 electrons in  $sp^3$  hybrids, corresponding to the first and second shells of bonds in (1), so the self-consistent calculation was carried out with 18 electrons fixed at the Watson sphere.

The self-consistent energy spectra of the clusters 8Si and 20Si are presented in Fig. 2. The energy

spectrum of a 17-atom cluster is also shown, for comparison: this model has been used in previous studies of point defects in Si,<sup>23</sup> GaAs,<sup>29</sup> and GaSb.<sup>32</sup> The energy levels are labeled according to the irreducible representations of the  $T_d$  point group and the calculations were performed with 36 electrons transferred to the Watson sphere. According to our way of treating the dangling bonds, the bulk band edges are determined assuming that the highest occupied and lowest unoccupied molecular orbitals correspond to the top of the valence band and to the bottom of the conduction band, respectively. For all clusters, the top of the valence band is placed at the zero of energy.

From Fig. 2 we can note that for the 8-atom cluster the valence-band orbital symmetries are exactly those predicted by group theory, as is the case also for the 17-atom cluster.<sup>23</sup> For the 20-atom cluster, we have an extra  $a_{2u}$  orbital, where we should have an  $a_{1u}$ . This can be explained

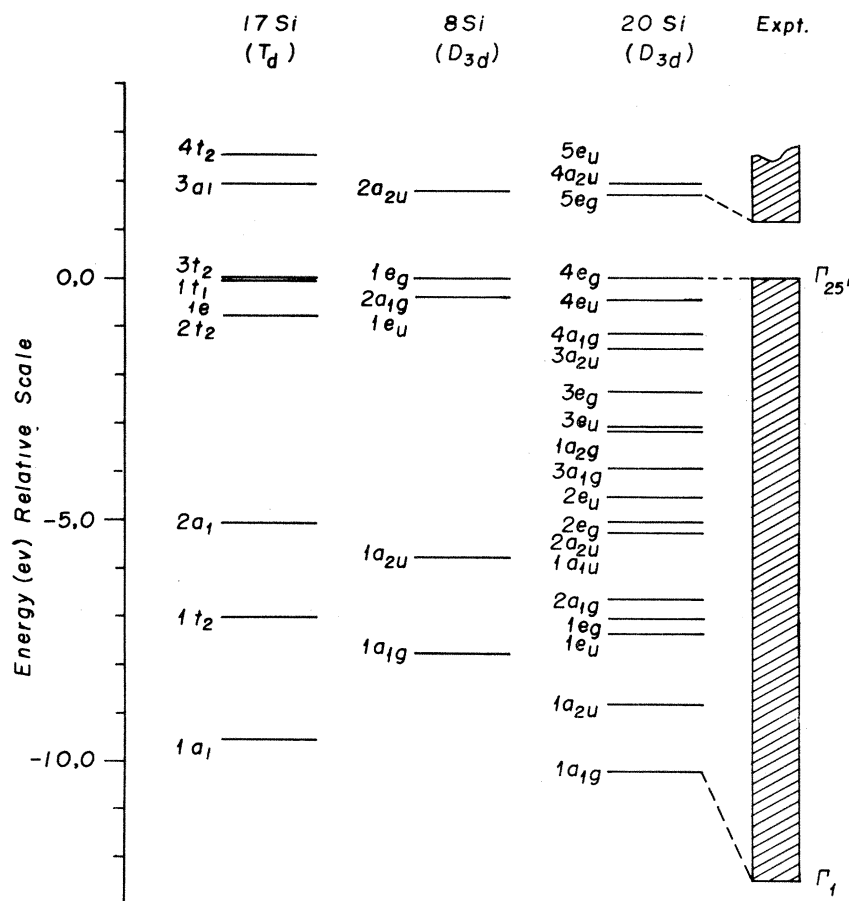


FIG. 2. Energy spectra of the clusters 17Si, 8Si, and 20Si, simulating the electronic structure of the Si crystal. The symmetry of each cluster is indicated. The experimental values for the valence-band width and band gap are shown (Ref. 30).

bearing in mind that the six atoms of the second shell are not completely saturated by the atoms of the third shell, so that we have a number of dangling bonds in an inner shell of the cluster. This fact caused an  $a_{2u}$  surface orbital to be mixed up with the valence-band states, and forced out an  $a_{1u}$  orbital which ended up at 1.17 eV above the highest occupied  $e_g$  orbital. This latter state should rightly be inside the valence band, and must not be treated on equal footing with the other unoccupied orbitals; in particular, this state cannot be used to define the bottom of the conduction band. Accordingly, this orbital is not shown in the figures, and is left unoccupied when we study the defects in Sec. II 3. It should be remarked, however, that the state really behaves as a bulk state, remaining stationary in energy throughout the defect implantations, with charge distribution virtually unchanged.

The symmetry of the uppermost occupied energy level is  $e_g(t_2)$  and corresponds to the top of the bulk-valence band ( $\Gamma_{25'}$ ), according to the energy spectra of the clusters of  $D_{3d}(T_d)$  symmetry. The bottom of the valence band ( $\Gamma_1$ ) is defined by the  $1a_{1g}(1a_1)$  energy level according to the  $D_{3d}(T_d)$  symmetry. Figure 2 shows that the lowest unoccupied energy levels are the  $3a_1$ ,  $2a_{2u}$ , and  $5e_g$  for the clusters 17Si, 8Si, and 20Si, respectively; according to our model, they define the bottom of the conduction band.

The numerical values for the crystal band gap and valence-band width obtained for the clusters are shown in Table I. The experimental data, quoted in Ref. 47, are included for comparison. The entries were determined through one-electron energy differences (Koopman's method), neglecting the molecular orbital relaxation effects. By use of the transition-state concept<sup>22</sup> it was found that these effects are negligible as far as the value for the band gap is concerned. From Fig. 2 and Table I we can verify that the molecular cluster model

yields the main features of the bulk electronic structure. The energy bands of Si have been extensively calculated assuming several approximations to the crystal potential and to the exchange-correlation energy<sup>30</sup>; in spite of these attempts to reproduce the experimental data, the best results are still obtained through empirical pseudopotential methods. Thus, it is gratifying to see that the small clusters used depict realistically the band gap and valence-band width of Si.

### B. Si:P<sub>2</sub> and Si:P<sub>2</sub><sup>+</sup> complexes

In Fig. 3 are shown the energy spectra of the clusters 20Si, 18Si + P<sub>2</sub>, and 18Si + P<sub>2</sub><sup>+</sup>, corresponding to the electronic structure of the bulk and the Si:P<sub>2</sub> and Si:P<sub>2</sub><sup>+</sup> complexes. For the positively charged complex, the calculations were carried out to the spin-polarized limit.

The band edges are defined from the energy levels of the 20Si cluster. When the two atoms of the first shell are replaced by two P atoms, the band edges are affected due to the lower density of states in the finite cluster, so, in order to locate the impurity levels with respect to the bulk structure, we follow the prescription used in our previous works. We identify one or more molecular orbitals which correspond to a bulk valence state and take the related energy levels as reference to define the band edges for the complexes. The *s* and *p* atomic orbitals of the atoms of the first shell do not contribute to a molecular orbital of  $a_{1u}$  or  $a_{2g}$  symmetry. On the other hand, the corresponding charge distributions for the  $1a_{2g}$  and  $1a_{1u}$  levels remain virtually unaltered when the Si atoms are replaced by the P atoms. Thus, these energy levels are used as reference to compare the spectra in Fig. 3. However, it is worth mentioning that the energy shifts involved in the assignment of the same value for

TABLE I. Comparison of theoretical and experimental energies for Si. All entries are in eV.

	17Si ( $T_d$ )	8Si ( $D_{3d}$ )	20Si ( $D_{3d}$ )	Experiment <sup>a</sup>
Band gap	1.96	1.78	1.70	1.13, 4.15 <sup>b</sup>
Valence-band width	9.60	7.77	10.23	12.4±0.6

<sup>a</sup>Reference 30.

<sup>b</sup>Gap at  $\Gamma$  point (direct).

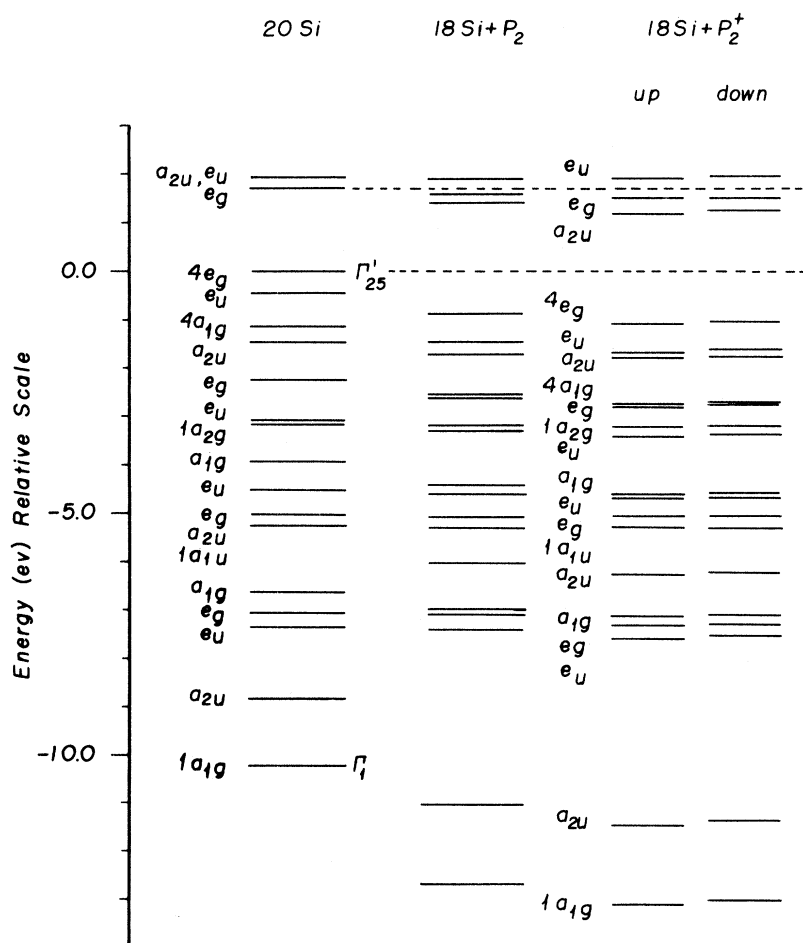


FIG. 3. Energy spectra of the clusters  $20\text{Si}$ ,  $18\text{Si} + \text{P}_2$ , and  $18\text{Si} + \text{P}_2^+$ , simulating the electronic structures of the  $\text{Si}$ ,  $\text{Si:P}_2$ , and  $\text{Si:P}_2^+$  systems, respectively. The dashed lines indicate the crystal band gap.

the  $1a_{2g}$  and  $1a_{1u}$  levels in the spectra are very small and, as can be seen from the figure, the spacing between them is not affected.

According to Fig. 3, the  $\text{P}_2$  and  $\text{P}_2^+$  impurities introduce a nondegenerate,  $a_{2u}$ , and a twofold degenerate,  $e_g$ , impurity level within the band gap. The  $a_{2u}$  level is fully occupied in the  $18\text{Si} + \text{P}_2$  cluster, and has one electron in the  $18\text{Si} + \text{P}_2^+$  cluster. One finds that in the positive charge state of the defect, the impurity levels move down within the band gap.

The overall analysis of the charge distribution in the clusters leads to the conclusion that the  $s$  and  $p$  atomic orbitals of the P atoms overlap and reconstruct the chemical bonds with the Si atoms of the second shell. In Table II we show the charge distributions for the  $1a_{1g}$  and  $4e_g$  states of the clusters. These states define the bottom and top of the valence band in the  $20\text{Si}$  cluster, and the associated

charge distributions are quite the same in the three clusters. They are expected to have lower energy in the complexes since the  $3s$  and  $3p$  levels are deeper in the P atom than the corresponding levels in the Si atom. As we see from Table II, the  $1a_{1g}$  and  $4e_g$  states correspond to charge distributions slightly more concentrated in the first shell of P atoms. This also is to be expected, since the  $1a_{1g}$  state is mainly formed from the phosphorus (Si)  $s$  orbitals and the  $4e_g$  state is mainly formed from the phosphorus (Si)  $p$  orbitals. The two extra electrons provided by the P atoms occupy the  $a_{2u}$  molecular orbital, which has a strong contribution from the phosphorus  $p$  atomic orbitals. This impurity level is related to a charge distribution with significant values in the three shells of atoms in the clusters. Thus, our results show that the complexes analyzed here give rise to impurity states which do not correspond to broken bonds.

TABLE II. Charge distributions normalized to one electron for the "valence states"  $1a_{1g}$  and  $4e_g$  of the clusters. The charge in the interatomic region was evenly distributed among the muffin-tin atomic spheres. The charge in the extramolecular region has negligible values.

Cluster	Orbital	First shell (species)	Second shell (species)	Third shell (species)
		(Si)	(Si)	(Si)
20Si	$1a_{1g}$	0.624	0.280	0.095
	$4e_g$	0.280	0.462	0.262
		(P)	(Si)	(Si)
18Si + P <sub>2</sub>	$1a_{1g}$	0.796	0.142	0.061
	$4e_g$	0.301	0.359	0.339
		(P)	(Si)	(Si)
18Si + P <sub>2</sub> <sup>+</sup>	$1a_{1g}\uparrow$	0.790	0.147	0.062
	$4e_g\uparrow$	0.315	0.366	0.317

### III. COMPARISON WITH EPR EXPERIMENTS

In this section we compare the results of our calculations with EPR measurements performed on heavily P-doped Si, irradiated at room temperature with 1.5-MeV electrons.<sup>25</sup> According to Sieverts, three new EPR spectra could be identified as two-phosphorus defect complexes. They show a hyperfine structure associated to complexes with electron spin  $S = \frac{1}{2}$  in which two atoms with nuclear spin  $I = \frac{1}{2}$  are involved. One of these spectra, labeled NL3, is tentatively ascribed to a nearest-neighbor substitutional pair of P atoms, in its positive charge state. There are other well-established P-related defect models, such as the phosphorus-vacancy complex or phosphorus itself; however, the identification of the Si:P<sub>2</sub><sup>+</sup> complex from the NL3 spectrum is still a speculation. A large hyperfine interaction with the <sup>31</sup>P atom is found, resulting in a value of 150 MHz for the Fermi contact term. To interpret the data the author uses a linear combination of atomic orbitals representation of the electron wave function, and within this model 3.2% of the charge density is located on the first shell of P atoms. Furthermore the NL3 spectrum indicates a C<sub>1h</sub> or C<sub>2h</sub> symmetry for the stabilized complex.

According to our calculations, the detected EPR spectrum NL3 may be related to the  $a_{2u}$  impurity state found in the electronic structure of the 18Si + P<sub>2</sub><sup>+</sup> cluster. The impurity level is occupied by single electron, implying that the cluster is an

open-shell system with  $S = \frac{1}{2}$ . In Table III, we show the charge distribution normalized to one electron for the  $a_{2u}$  state of Si:P<sub>2</sub> and Si:P<sub>2</sub><sup>+</sup> complexes. Although the  $a_{2u}$  impurity level lies deeper in the band gap for the Si:P<sub>2</sub><sup>+</sup> complex, the charge distributions are quite similar in both clusters. Moreover, there is a rather large charge concentration in the first shell of P atoms, with a value of 39% for the Si:P<sub>2</sub><sup>+</sup> system. Therefore, a strong hyperfine interaction with the <sup>31</sup>P is expected, and indeed a value of about 800 MHz was calculated for the Fermi contact term. The main contribution to this value comes from the impurity state itself, since the spin-polarization effects yield negligible contributions to the magnetic hyperfine field.

We note that the ground state of the 18Si + P<sub>2</sub><sup>+</sup> cluster is a nondegenerate electronic state, so the system does not undergo a normal Jahn-Teller (JT) distortion. However, we must bear in mind that the  $a_{2u}$  and  $e_g$  energy levels are close enough to each other in the band gap to allow for a second-order JT (pseudo-JT) effect. The non-null off-diagonal matrix elements correspond to normal modes of  $E_u$  ( $A_{2u} \otimes E_g$ ) symmetry. The vibrational mode  $e_u$  removes the degeneracy of the  $e_g$  level and lowers the symmetry of the complex from  $D_{3d}$  to  $C_{1h}$ . The charge redistribution that follows a distortion may explain the discrepancy between the calculated result for the contact magnetic field and the experimental value.

The defect model depicted by our calculations, including the pseudo-JT - effect, explains some

TABLE III. Charge distributions normalized to one electron for the impurity state  $a_{2u}$  of the Si:P<sub>2</sub> and Si:P<sub>2</sub><sup>+</sup> complexes. The charge in the interatomic region was evenly distributed among the muffin-tin atomic spheres. The charge in the extramolecular region has negligible values.

Complex	Orbital (occupancy)	First shell P	Second shell Si	Third shell Si
Si:P <sub>2</sub>	$a_{2u}(2)$	0.348	0.391	0.260
Si:P <sub>2</sub> <sup>+</sup>	$a_{2u_1}(1)$	0.394	0.351	0.255
	$a_{2u_1}(0)$	0.392	0.248	0.360

features of the NL3 spectrum reported by Sieverts. However, for a precise characterization of the Si:P<sub>2</sub><sup>+</sup> system and a fair comparison between theory and experiment, more work on both fields is necessary. For example, the activation energy of the center can be checked against the calculated value for the ionization energy of the impurity level.

From the results reported in this work we may conclude that, contrary to most effects of high doping on semiconductors, the formation and behavior of the double- and single-donor systems Si:P<sub>2</sub> and Si:P<sub>2</sub><sup>+</sup> cannot be analyzed within the

context of the effective-mass theory. The impurity levels seem to be related to rather localized wave functions in the vicinity of the defect.

#### ACKNOWLEDGMENTS

The authors are very grateful to Professor C. A. J. Ammerlaan for his interest, suggestions, encouragement, and for many helpful discussions. This work has been supported by the Fundação de Amparo à Pesquisa do Estado de São Paulo.

- <sup>1</sup>J. W. Corbett, J. C. Bourgoin, L. J. Cheng, J. C. Corelli, Y. H. Lee, P. M. Mooney, and C. Weigel, in *International Conference on Radiation Effects in Semiconductors, Dubrovnik, 1976*, edited by N. B. Urli and J. W. Corbett (IOP, Bristol, 1977), p. 1, and references therein.
- <sup>2</sup>S. T. Pantelides, *Rev. Mod. Phys.* **50**, 797 (1978), and references therein.
- <sup>3</sup>V. F. Masterov and B. E. Samorukov, *Fiz. Tekh. Poluprovodn.* **12**, 625 (1978) [*Sov. Phys.—Semicond.* **12**, 363 (1978)], and references therein.
- <sup>4</sup>M. Jaros, *Adv. Phys.* **29**, 409 (1980).
- <sup>5</sup>R. N. Bhatt and T. M. Rice, *Phys. Rev. B* **23**, 1920 (1981).
- <sup>6</sup>J. Allègre and M. Avérous, in *International Conference on Radiation Effects in Semiconductors, Nice, 1978*, edited by J. H. Albany (IOP, London, 1979), p. 379.
- <sup>7</sup>G. D. Watkins, in *Lattice Defects in Semiconductors—1974*, edited by F. A. Huntley (IOP, London, 1975), p. 1.
- <sup>8</sup>E. L. Elkins and G. D. Watkins, *Phys. Rev.* **174**, 881 (1968).
- <sup>9</sup>R. Z. Bachrach, D. G. Lorimar, L. R. Dowson, and K. B. Wolfstern, *J. App. Phys.* **43**, 5098 (1972).
- <sup>10</sup>J. G. de Wit, E. G. Sieverts, and C. A. J. Ammerlaan, *Phys. Rev. B* **14**, 3494 (1976).
- <sup>11</sup>E. G. Sieverts, S. H. Muller, and C. A. J. Ammerlaan, *Phys. Rev. B* **18**, 6834 (1978).
- <sup>12</sup>G. A. Thomas, M. Capizzi, F. De Rosa, R. N. Bhatt, and T. M. Rice, *Phys. Rev. B* **23**, 5472 (1981), and references therein.
- <sup>13</sup>J. Golka and H. Stoll, *Solid State Commun.* **33**, 1183 (1980).
- <sup>14</sup>T. F. Lee and T. C. McGill, *J. Phys. C* **6**, 3438 (1973).
- <sup>15</sup>V. A. Singh, C. Weigel, J. W. Corbett, and L. M. Roth, *Phys. Status Solidi B* **81**, 637 (1977).
- <sup>16</sup>C. A. J. Ammerlaan and J. C. Wolfrat, *Phys. Status Solidi B* **89**, 85 (1978).
- <sup>17</sup>M. Vandevyver and D. N. Talwar, *Phys. Rev. B* **21**, 3405 (1980), and references therein.
- <sup>18</sup>J. E. Lowther, *J. Phys. C* **10**, 2501 (1977).
- <sup>19</sup>O. F. Sankey, H. P. Hjalmarsen, J. D. Dow, D. J. Wolford, and B. G. Streetman, *Phys. Rev. Lett.* **45**, 1656 (1980).
- <sup>20</sup>O. F. Sankey and J. D. Dow, *Appl. Phys. Lett.* **38**, 685 (1981).
- <sup>21</sup>M. Jaros and S. Brand, *Phys. Rev. B* **14**, 4494 (1976).
- <sup>22</sup>K. H. Johnson, *Annu. Rev. Phys. Chem.* **26**, 39

- (1975).
- <sup>23</sup>A. Fazzio, M. J. Caldas, and J. R. Leite, *Int. J. Quantum Chem.* **S13**, 394 (1979).
- <sup>24</sup>A. Fazzio, J. R. Leite, and M. L. De Siqueira, *J. Phys. C* **12**, 3469 (1979).
- <sup>25</sup>E. G. Sieverts, thesis, University of Amsterdam, 1978 (unpublished); E. G. Sieverts and C. A. J. Ammerlaan, in *International Conference on Radiation Effects in Semiconductors, Dubrovnik, 1976*, Ref. 1, p. 213.
- <sup>26</sup>L. A. Hemstreet, *Phys. Rev. B* **15**, 834 (1977).
- <sup>27</sup>G. G. De Leo, G. D. Watkins, and W. B. Fowler, *Phys. Rev. B* **23**, 1851 (1981).
- <sup>28</sup>A. C. Kenton and M. W. Ribarsky, *Phys. Rev. B* **23**, 2897 (1981).
- <sup>29</sup>A. Fazzio and J. R. Leite, *Phys. Rev. B* **21**, 4710 (1980).
- <sup>30</sup>F. Szmulowicz, *Phys. Rev. B* **23**, 1652 (1981).
- <sup>31</sup>K. Schwarz, *Phys. Rev. B* **5**, 2466 (1972).
- <sup>32</sup>L. M. Brescansin and A. Fazzio, *Phys. Status Solidi B* (in press).